

AD-A256 470



12

DIFFUSION PROBLEMS IN BONDED  
NONHOMOGENEOUS MATERIALS  
WITH AN INTERFACE CUT

DTIC  
ELECTE  
OCT 16 1992  
S C D

by  
Fazil Erdogan and Murat Ozturk

DISTRIBUTION STATEMENT A  
Approved for public release  
Distribution Unlimited

Lehigh University, Bethlehem, PA

August 1992

FINAL PROJECT REPORT

OFFICE OF NAVAL RESEARCH CONTRACT NO. N00014-89-3188

82 1 10 12

205450

DEFENSE TECHNICAL INFORMATION CENTER



9227276

5798

**DIFFUSION PROBLEMS IN BONDED  
NONHOMOGENEOUS MATERIALS  
WITH AN INTERFACE CUT**

by

**Fazil Erdogan and Murat Ozturk**

**Lehigh University, Bethlehem, PA**

**August 1992**

**FINAL PROJECT REPORT**

**OFFICE OF NAVAL RESEARCH CONTRACT NO. N00014-89-3188**

St-A per telecom, Mr. Rajatakse,  
ONR/Code 1132sm. Arl., VA.  
JK 10-16-92

DTIC Contract Number N00014-89-3188

Accession For	
NTIS GRA&I	<input checked="" type="checkbox"/>
DTIC TAB	<input type="checkbox"/>
Unannounced	<input type="checkbox"/>
Justification	
By	
Distribution/	
Availability Codes	
Avail and/or	
Dist	Special
A-1	

# DIFFUSION PROBLEMS IN BONDED NONHOMOGENEOUS MATERIALS WITH AN INTERFACE CUT

by

Fazil Erdogan and Murat Ozturk

Lehigh University, Bethlehem, PA 18015

## ABSTRACT

In this paper the mixed boundary value problem for a nonhomogeneous medium bonded to a rigid subspace is considered. The main objective is to investigate the techniques that would lead to analytically tractable solutions and to provide examples comparing the results of various kinds of material nonhomogeneities. The problem studied is a two dimensional diffusion problem in which the interface contains a plane crack. An elastic medium under antiplane shear loading is used to formulate the problem. However, the results may be interpreted in terms of any number of steady-state diffusion phenomena. The method used is essentially an inverse method in the sense that it provides the material constitutive behavior for which the mixed boundary value problem can be solved rather than solving the problem for a given material. Two different methods are described and some numerical examples are given.

### 1. Introduction

Increasing concerns in recent years with mechanical failure initiating at the interfacial regions in many technologically important multiphase materials require a better understanding of the interaction between flaws that may exist in these regions and the applied loads and other environmental factors. The conventional approach to studying the thermomechanics of such materials is based on the assumption that the composite medium is piecewise homogeneous and the flaws may be represented by plane cuts or cracks. On the other hand in most bonded materials the interfacial region appears to have a structure which is generally different than that of the adjacent materials. In many cases, such as in plasma spray coating, sputtering, ion plating and in some diffusion bonded materials, the thermomechanical properties of the region are "graded" in the sense that the interfacial region is a nonhomogeneous continuum of

finite thickness with very steep property gradients [1], [2]. Among other applications of bonded nonhomogeneous materials one may mention certain geophysical materials with naturally graded compositions such as shale/sandstone and materials which have highly temperature dependent properties and are under steep temperature gradients. However, perhaps the most important reason for studying the diffusion and fracture problems in bonded nonhomogeneous materials is the technological potential of the so-called functionally gradient materials (FGM). These are the multiphase materials, interlayers and coatings synthesized in such a way that the volume fractions of the constituents are varied continuously in thickness direction to give a predetermined composition profile [3] - [9]. The material thus obtained is known to have some wide ranging highly desirable properties. From the viewpoint of failure mechanics some of these properties are reduced thermal stresses, residual stresses and stress concentration factors [3], improved bonding strength [6], and improved toughness and corrosion and fatigue crack growth resistance. Most of the current research on FGMs appears to be in the area of ceramic coatings motivated by a variety of thermal shielding problems and in growing superconducting or diamond films over homogeneous substrates [5].

The general problem of interest here is the heat diffusion and the fracture mechanics problems in a medium that consists of a nonhomogeneous layer bonded to a homogeneous substrate and contains an interface crack. The primary objective is to investigate the techniques which would lead to analytically tractable solutions of the related mixed boundary value problems and to provide some examples comparing the results of various kinds of material nonhomogeneities. To do this we consider a problem which is relatively simple to work with and yet has all the analytical features that need to be investigated. The problem studied here is a two-dimensional diffusion problem for a nonhomogeneous medium bonded to a rigid half space having a crack along the interface. Even though the terminology used will be that of an elasticity problem for a medium under antiplane shear loading, the results may be interpreted in terms of any number of diffusion phenomena.

## 2. Formulation of the Problem - A Direct Method

Consider the antiplane shear problem for a semi infinite nonhomogeneous elastic medium shown in Fig. 1. It is assumed that the medium is bonded to a rigid half space

along the  $y=0$  plane, the interface contains a crack on  $y=0$ ,  $-a < x < a$ , and the medium is subjected to arbitrary antiplane shear loading which may be mechanical or thermal in origin. It is also assumed that the problem is solved under actual loading conditions in the absence of a crack and through a proper superposition is reduced to a local perturbation problem in which the crack surface tractions are the only non-zero external loads. Furthermore, if we assume that the shear modulus  $\mu$  is a function of  $y$  only, the non-vanishing stress components and the equilibrium equation may be expressed as

$$\sigma_{xy} = \mu \frac{\partial w}{\partial x}, \quad \sigma_{yz} = \mu \frac{\partial w}{\partial y}, \quad (2.1)$$

$$\mu \nabla^2 w + \frac{\partial \mu}{\partial y} \frac{\partial w}{\partial y} = 0, \quad (2.2)$$

where  $w$  is the  $z$  component of the displacement vector. In the crack problem under consideration (2.2) will have to be solved under the following mixed boundary conditions:

$$\sigma_{yz}(x, 0) = \sigma_0(x), \quad -a < x < a$$

$$w(x, 0) = 0, \quad a < |x| < \infty, \quad (2.3)$$

$\sigma_0(x)$  being the known crack surface traction.

Let the solution of (2.2) be given by

$$w(x, y) = \frac{1}{2\pi} \int_{-\infty}^{\infty} F(y, \alpha) e^{-i\alpha x} d\alpha. \quad (2.4)$$

From (2.2) and (2.4) it follows that

$$\frac{d^2 F}{dy^2} + p(y) \frac{dF}{dy} - \alpha^2 F = 0 \quad (2.5)$$

where

$$p(y) = \frac{d}{dy} [\log \mu(y)] = \frac{\mu'(y)}{\mu(y)}. \quad (2.6)$$

If we replace the unknown function  $F$  by  $H$  so that

$$F(y, \alpha) = H(y, \alpha) \exp \left[ -\frac{1}{2} \int^y p(t) dt \right] = H(y, \alpha) (\mu(y))^{-\frac{1}{2}}, \quad (2.7)$$

equation (2.5) becomes

$$\frac{d^2 H}{dy^2} - \frac{1}{4} \left( p^2 + 2 \frac{dp}{dy} + 4\alpha^2 \right) H = 0. \quad (2.8)$$

We will now look for a particular class of functions  $\mu(y)$  for which (2.8) has an analytical solution. The simplest of such class of functions are obtained by assuming that

$$\frac{1}{2} \frac{dp}{dy} + \frac{1}{4} p^2 = c_0, \quad (2.9)$$

where  $c_0$  is a constant. Three classes of functions satisfying (2.9) may thus be obtained as follows:

$$(a) \quad c_0 = \beta^2 :$$

$$p(y) = \mp 2\beta, \quad \mu(y) = \mu_0 \exp(\mp 2\beta y), \quad (2.10)$$

$$p(y) = 2\beta \coth(\beta y + \delta), \quad \mu(y) = \mu_0 \sinh^2(\beta y + \delta), \quad (2.11)$$

$$p(y) = 2\beta \tanh(\beta y + \delta), \quad \mu(y) = \mu_0 \cosh^2(\beta y + \delta); \quad (2.12)$$

$$(b) \quad c_0 = -\beta^2 :$$

$$p(y) = -2\beta \tan(\beta y + \delta), \quad \mu(y) = \frac{\mu_0}{\cos^2(\beta y + \delta)}, \quad (2.13)$$

$$p(y) = 2\beta \cot(\beta y + \delta), \quad \mu(y) = \mu_0 \sin^2(\beta y + \delta); \quad (2.14)$$

$$(c) \quad c_0 = 0 :$$

$$p(y) = 0, \quad \mu(y) = \mu_0, \quad (2.15)$$

$$p(y) = \frac{2\beta}{\beta y + \delta}, \quad \mu(y) = \mu_0 (\beta y + \delta)^2, \quad (2.16)$$

where  $\beta$ ,  $\delta$ , and  $\mu_0$  are arbitrary constants ( $\mu_0 > 0$ ).

From (2.8) and (2.9) it is seen that

$$\frac{d^2 H}{dy^2} - \lambda^2 H = 0, \quad \lambda^2 = \alpha^2 + c_0, \quad \lambda = (\alpha^2 + c_0)^{1/2}. \quad (2.17)$$

Formally, from (2.4), (2.11) and (2.17) we now obtain

$$w(x, y) = \frac{1}{2\pi} \left( \frac{\mu(y)}{\mu_0} \right)^{1/2} \int_{-\infty}^{\infty} A(\alpha) \exp(-\lambda y - i\alpha x) d\alpha, \quad (2.18)$$

where the constant  $\mu_0$  is introduced for dimensional considerations and the function  $A$  is unknown to be determined from (2.3). The physics of the problem requires that  $w \rightarrow 0$  for  $y \rightarrow \infty$ . Thus, from (2.17) and (2.18) it may be observed that  $\lambda$  defined by  $\lambda = (\alpha^2 + c_0)^{1/2}$  must be positive for all values of  $\alpha$  and, therefore, the negative values of  $c_0$  or shear moduli given by (2.13) and (2.14) would not be acceptable for the solution expressed by (2.18). From (2.1) and (2.15) the stress components are found to be

$$\sigma_{xz} = -\frac{\mu}{2\pi} \left( \frac{\mu(y)}{\mu_0} \right)^{-1/2} \int_{-\infty}^{\infty} i\alpha A(\alpha) \exp(-\lambda y - i\alpha x) d\alpha, \quad (2.19)$$

$$\sigma_{yz} = -\frac{1}{2\pi} \left( \frac{\mu_0}{\mu(y)} \right)^{1/2} \int_{-\infty}^{\infty} \left( \lambda\mu + \frac{1}{2}\mu' \right) A(\alpha) \exp(-\lambda y - i\alpha x) d\alpha. \quad (2.20)$$

By substituting from (2.18) and (2.20) into (2.3) one would obtain a pair of dual integral equations to determine  $A(\alpha)$ . The problem may also be reduced to an integral equation by defining

$$\frac{\partial}{\partial x} w(x, 0) = g(x). \quad (2.21)$$

From (2.3b), (2.18) and (2.21) it may thus be seen that

$$\left( \frac{\mu_0}{\mu(0)} \right)^{1/2} i\alpha A(\alpha) = - \int_{-a}^a g(t) e^{i\alpha t} dt. \quad (2.22)$$

Substituting now from (2.20) and (2.22) into (2.3a) we obtain

$$\lim_{y \rightarrow +0} \frac{1}{2\pi} \int_{-a}^a g(t) dt \int_{-\infty}^{\infty} K(y, \alpha) e^{i\alpha(t-x)} d\alpha = \sigma_{yz}(x, 0) = \sigma_0(x), \quad -a < x < a \quad (2.23)$$

where

$$K(y, \alpha) = \frac{\lambda\mu(y) + \mu'(y)/2}{i\alpha} e^{-\lambda y}. \quad (2.24)$$

To investigate and to separate a possible singular part of the kernel in (2.23), the asymptotic behavior of the inner integral for  $|\alpha| \rightarrow \infty$  must be examined. From (2.17) it is seen that  $\lambda \rightarrow |\alpha|$  for  $|\alpha| \rightarrow \infty$ . Thus, for  $|\alpha| \rightarrow \infty$  from (2.24) we obtain

$$K_\infty(y, \alpha) = \frac{\mu(y)}{i} \frac{|\alpha|}{\alpha} e^{-|\alpha|y}. \quad (2.25)$$

By adding and subtracting  $K_\infty$  in (2.23) and by observing that

$$\int_{-\infty}^{\infty} \frac{1}{i} \frac{|\alpha|}{\alpha} e^{-|\alpha|y} e^{i\alpha(t-x)} d\alpha = \frac{2(t-x)}{(t-x)^2 + y^2}, \quad (2.26)$$

from (2.23) we obtain

$$\frac{1}{\pi} \int_{-a}^a \left[ \frac{1}{t-x} + k(x, t) \right] g(t) dt = \frac{\sigma_0(x)}{\mu(0)}, \quad -a < x < a, \quad (2.27)$$

$$k(x, t) = \frac{1}{2} \int_{-\infty}^{\infty} \left( \frac{2\lambda + \mu'(0)/\mu(0)}{2i\alpha} - \frac{|\alpha|}{i\alpha} \right) e^{i\alpha(t-x)} d\alpha, \quad (2.28)$$

where the kernel  $k(x, t)$  is bounded in the closed interval  $-a \leq (x, t) \leq a$ .

From (2.3b) and (2.21) it follows that (2.27) must be solved under the following single-valuedness condition:

$$\int_{-a}^a g(t) dt = 0. \quad (2.29)$$

### 3. Method of Embedding

Even though the direct method used in the previous section yields only a limited choice for representing the shear modulus  $\mu(y)$ , keeping in mind that the mixed boundary value problems which are of practical interest tend to be generally local perturbation problems, it may not be difficult to approximate  $\mu(y)$  with sufficient

accuracy in the region of interest by using the representations (2.10), (2.11), (2.12) or (2.16). To solve the problem one could also follow the technique developed by Varley and Seymour [10] for transforming partial differential equations with variable coefficients into equations with constant coefficients. The technique is more general in scope but also is more complicated. Following [10] we first replace the equilibrium equation (2.2) by

$$\mu(y) \frac{\partial w}{\partial x} = \frac{\partial f}{\partial y}, \quad \mu(y) \frac{\partial w}{\partial y} = -\frac{\partial f}{\partial x}. \quad (3.1)$$

Introducing the functions  $W(x,y)$  and  $F(x,y)$  which satisfy

$$\frac{\partial W}{\partial x} = \frac{\partial F}{\partial y}, \quad \frac{\partial W}{\partial y} = -\frac{\partial F}{\partial x}, \quad (3.2)$$

we now express  $w$  and  $f$  in terms of  $W(x,y)$ ,  $F(x,y)$  and a system of coefficient functions  $w_n(y)$  and  $f_n(y)$  as follows:

$$w(x,y) = \sum_0^N w_n(y) \frac{\partial^{N-n}}{\partial y^{N-n}} W, \quad (3.3a)$$

$$f(x,y) = \sum_0^N f_n(y) \frac{\partial^{N-n}}{\partial y^{N-n}} F. \quad (3.3b)$$

Substituting from (3.3) into (3.1) and using (3.2) we obtain

$$f_0 \frac{\partial^N}{\partial y^N} \left( \frac{\partial W}{\partial y} \right) + \sum_1^N f_n \frac{\partial^{N-n}}{\partial y^{N-n}} \left( \frac{\partial W}{\partial y} \right) = \mu w_0 \frac{\partial^N}{\partial y^N} \left( \frac{\partial W}{\partial y} \right) + \mu \sum_1^N (w_n + w'_{n-1}) \frac{\partial^{N-n}}{\partial y^{N-n}} \left( \frac{\partial W}{\partial y} \right) + \mu w'_N W,$$

$$\mu w_0 \frac{\partial^N}{\partial y^N} \left( \frac{\partial W}{\partial x} \right) + \mu \sum_1^N w_n \frac{\partial^{N-n}}{\partial y^{N-n}} \left( \frac{\partial W}{\partial x} \right) = f_0 \frac{\partial^N}{\partial y^N} \left( \frac{\partial W}{\partial x} \right) + \sum_1^N (f_n + f'_{n-1}) \frac{\partial^{N-n}}{\partial y^{N-n}} \left( \frac{\partial W}{\partial x} \right) + w'_N F. \quad (3.4a,b)$$

An admissible set of functions,  $\mu$ ,  $f_n$  and  $w_n$  satisfying (3.4) may be obtained from

$$\begin{aligned}
 f_0 &= \mu w_0, \\
 f_n &= \mu w_n + \mu w'_{n-1}, \quad n = 1, \dots, N, \\
 w'_N &= 0, \\
 \mu w_n &= f_n + f'_{n-1}, \quad n = 1, \dots, N, \\
 f'_N &= 0.
 \end{aligned} \tag{3.5}$$

From (3.5) it may be shown that

$$\begin{aligned}
 w_0(y) &= \frac{1}{\sqrt{\mu'(y)}}, \quad f_0(y) = \sqrt{\mu'(y)}, \\
 w_N &= K_N, \quad f_N = L_N,
 \end{aligned} \tag{3.6}$$

where  $K_N$  and  $L_N$  are constant.

Equation (3.2) indicates that  $W$  is a harmonic function which, for  $y > 0$ ,  $-\infty < x < \infty$  may be expressed as

$$W(x, y) = \frac{1}{2\pi} \int_{-\infty}^{\infty} A(\alpha) e^{-|\alpha|y - i\alpha x} d\alpha, \tag{3.7}$$

From (3.3) and (3.7) it follows that

$$w(x, y) = \frac{1}{2\pi} \int_{-\infty}^{\infty} A(\alpha) H(y, \alpha) e^{-|\alpha|y - i\alpha x} d\alpha \tag{3.8}$$

where

$$H(y, \alpha) = \sum_0^N w_n(y) (-|\alpha|)^{N-n}. \tag{3.9}$$

If we again define  $g(t)$  by (2.21), from (2.3) and (3.8) we obtain

$$\begin{aligned}
& -\lim_{y \rightarrow 0^+} \frac{\mu(y)}{2\pi} \int_{-a}^a g(t) dt \int_{-\infty}^{\infty} \left( \frac{\partial H}{\partial y} - |\alpha| H \right) \frac{e^{-|\alpha|y + i\alpha(t-x)}}{i\alpha H(0, \alpha)} d\alpha \\
& = \sigma_{y,z}(x, 0) = \sigma_0(x), \quad -a < x < a.
\end{aligned} \tag{3.10}$$

By separating the singular kernel, from (3.10) and (3.9) it may be shown that

$$\lim_{y \rightarrow 0^+} \frac{1}{2\pi} \int_{-a}^a h(x, y, t) g(t) dt = \frac{\sigma_0(x)}{\mu(0)}, \quad -a < x < a, \tag{3.11}$$

$$\begin{aligned}
h(x, y, t) &= \frac{2w_0(y)}{w_0(0)} \frac{t-x}{(t-x)^2 + y^2} - \int_{-\infty}^{\infty} (K - K_\infty) e^{-|\alpha|y + i\alpha(t-x)} d\alpha, \\
K(y, \alpha) &= \frac{|\alpha| H - \frac{\partial H}{\partial y}}{i\alpha H(0, \alpha)}, \quad K_\infty(y, \alpha) = \frac{w_0(y)}{w_0(0)} \frac{|\alpha|}{\alpha}.
\end{aligned} \tag{3.12}$$

By taking the limit (3.11) becomes

$$\frac{1}{\pi} \int_{-a}^a \left\{ \frac{1}{t-x} + k_c(x, t) \right\} g(t) dt = \frac{\sigma_0(x)}{\mu(0)}, \quad -a < x < a, \tag{3.13}$$

where the kernel  $k_c$  is bounded in  $-a \leq (x, t) \leq a$  and is given by

$$\begin{aligned}
k_c(x, t) &= -\frac{1}{2} \int_{-\infty}^{\infty} \frac{\sum_0^N w_n'(0) (-|\alpha|)^{N-n}}{i\alpha \sum_0^N w_n(0) (-|\alpha|)^{N-n}} e^{i\alpha(t-x)} d\alpha \\
&= -\int_0^{\infty} \frac{\sum_0^N w_n'(0) (-\alpha)^{N-n}}{\alpha \sum_0^N w_n(0) (-\alpha)^{N-n}} \sin \alpha(t-x) d\alpha.
\end{aligned} \tag{3.14}$$

Equation (3.13) is again subject to the condition (2.29).

As an example consider the case of  $N = 1$ . From (3.5) and (3.6) it may be seen that

$$w_1 = K_1 \cdot f_1 = L_1, \quad (3.15)$$

$$\frac{df_0}{dy} = K_1 f_0^2 - L_1, \quad (3.16)$$

where  $K_1$  and  $L_1$  are arbitrary constants. The solution of (3.16) may be obtained as

$$K_1 L_1 > 0 :$$

$$f_0 = -\sqrt{\frac{L_1}{K_1}} \coth\left(L_1 \sqrt{\frac{K_1}{L_1}} (y + y_1)\right),$$

$$f_0 = -\sqrt{\frac{L_1}{K_1}} \tanh\left(L_1 \sqrt{\frac{K_1}{L_1}} (y - y_1)\right); \quad (3.17)$$

$$K_1 L_1 < 0 :$$

$$f_0 = -\sqrt{\left|\frac{L_1}{K_1}\right|} \tan\left(L_1 \sqrt{\left|\frac{K_1}{L_1}\right|} (y + y_1)\right),$$

$$f_0 = -\sqrt{\left|\frac{L_1}{K_1}\right|} \cot\left(L_1 \sqrt{\left|\frac{K_1}{L_1}\right|} (y + y_1)\right); \quad (3.18)$$

$$K_1 = 0 : f_0 = -L_1 (y + y_1); \quad (3.19)$$

$$L_1 = 0 : f_0 = -\frac{1}{K_1 (y + y_1)}. \quad (3.20)$$

From (3.6) observing that  $f_0 = \sqrt{\mu}$ , (3.17) - (3.20) now provides four different functional forms for which the mixed boundary value problem under consideration would be analytically tractable. For example, assuming  $L_1 = -\beta\sqrt{\mu_0}/\tanh\delta$ ,  $K_1 = -\beta\tanh\delta/\sqrt{\mu_0}$  and  $y_1 = \delta$ , from (3.17b) we find

$$f_0(y) = \sqrt{\mu(y)} = \sqrt{\mu_0} \tanh(\beta y + \delta)/\tanh\delta, \quad (3.21)$$

$$w_0(y) = \frac{1}{\sqrt{\mu(y)}} = \frac{1}{\sqrt{\mu_0}} \coth(\beta y + \delta)/\coth\delta. \quad (3.22)$$

Also, the Fredholm kernel given by (3.14) becomes

$$k_c(x,t) = 2\beta [\coth^2(\delta) - 1] \int_0^\infty \frac{\sin \alpha(t-x)}{\beta + \alpha \coth(\delta)} d\alpha . \quad (3.23)$$

It is clear that solutions for  $\mu(y)$  with greater number of arbitrary constants may be obtained from (3.5) by considering cases for which  $N > 1$  [10]. Technically the greater number of arbitrary constants would provide a better representation of the given shear modulus.

#### 4. Examples

We first consider the application of the method described in Section 2 and give two examples where we assume that  $c_0 > 0$  or  $c_0 = 0$  (see equations (2.9) - (2.16)). Thus, we let the shear modulus have the form

$$(a) \mu(y) = \mu_0 e^{2\beta y} , y \geq 0. \quad (4.1)$$

$$(b) \mu(y) = \mu_0(\beta y + \delta)^2 , y \geq 0 . \quad (4.2)$$

where  $\beta$  may be positive or negative. For the two cases (4.1) and (4.2) the Fredholm kernel expressed by (2.28) becomes

$$k_a(x,t) = \frac{\pi\beta}{2} \frac{|t-x|}{t-x} + \beta^2 \int_0^\infty \frac{\sin \alpha(t-x)}{\alpha(\alpha + \sqrt{\alpha^2 + \beta^2})} d\alpha . \quad (4.3)$$

$$k_b(x,t) = \frac{\beta}{\delta} \int_0^\infty \frac{\sin \alpha(t-x)}{\alpha} d\alpha = \frac{\pi}{2} \frac{\beta}{\delta} \frac{|t-x|}{t-x} . \quad (4.4)$$

From (2.27) and (2.28) it may be observed that the dominant part of the integral equation has only a Cauchy singularity. Consequently the solution of (2.27) has the form [11]

$$g(t) = \frac{G(t)}{\sqrt{a^2 - t^2}} , -a < t < a , \quad (4.5)$$

where  $G$  is unknown which is bounded in  $-a \leq t \leq a$  and non-zero at  $t = \mp a$ .

The integral equation (2.27) is solved numerically by normalizing the interval

and by observing that its fundamental function is the weight of Chebyshev polynomials  $T_n(s)$ . Thus, defining

$$t = as, \quad x = ar, \quad g(t) = o(s) = \frac{h(s)}{\sqrt{1-s^2}}, \quad h(s) = \frac{G(as)}{a}, \quad (4.6)$$

The unknown function  $h(s)$  may be expressed as

$$h(s) = \frac{1}{\mu(0)} \sum_0^{\infty} A_n T_{2n-1}(s) \quad (4.7)$$

where  $A_0, A_1, \dots$  are unknown constants and only the symmetric loading is considered, that is,  $\sigma_0(x) = \sigma_0(-x)$  and  $w(x, y) = w(-x, y)$ . By using the following properties of Chebyshev polynomials

$$\frac{1}{\pi} \int_{-1}^1 \frac{T_n(s) ds}{(s-r)\sqrt{1-s^2}} = \begin{cases} 0, & n=0, \quad -1 < r < 1, \\ U_{n-1}(r), & n=1, 2, \dots, \quad -1 < r < 1, \\ -\frac{|r|/r}{\sqrt{r^2-1}} \left[ r - (|r|/r) \sqrt{r^2-1} \right]^n, & n=0, 1, \dots, \quad |r| > 1 \end{cases} \quad (4.8)$$

and by substituting from (4.6) and (4.7) into (2.27) we obtain

$$\sum_0^{\infty} A_n [U_{2n-2}(r) + M_{2n-1}(r)] = \sigma_0(ar), \quad -1 < r < 1, \quad (4.9)$$

$$M_{2n-1}(r) = \frac{1}{\pi} \int_{-1}^1 a \left\{ \begin{array}{l} k_a(ar, as) \\ k_b(ar, as) \end{array} \right\} \frac{T_{2n-1}(s)}{\sqrt{1-s^2}} ds. \quad (4.10)$$

Also, by using the orthogonality conditions of  $T_n(s)$  from (2.29), (4.6) and (4.7) it follows that

$$A_0 = 0. \quad (4.11)$$

The simplest way of solving the functional equation (4.9) without sacrificing accuracy appears to be truncating the series at  $n = N$  and using an appropriate

collocation technique. In this case because of the nature of the problem it is necessary to increase the density of the collocation points near the singular points  $r = \mp 1$ . Thus, these points may be selected as follows:

$$T_N(r_i) = 0, \quad r_i = \cos\left[\frac{\pi}{2N}(2i-1)\right], \quad i = 1, \dots, N. \quad (4.12)$$

The linear algebraic equations obtained from (4.9) by substituting  $r = r_i, i = 1, \dots, N$  would then give the unknown coefficients  $A_1, \dots, A_N$ .

One may note that in case (b) the kernel  $k_b$  is known in closed form and by using (4.4) and (4.10) the functional equation (4.9) may further be simplified as follows:

$$\sum_1^{\infty} A_n \left[ U_{2n-2}(r) + \frac{\lambda}{2n-1} \sin(2n-1)\theta \right] = \sigma_0(r), \quad -1 < r < 1, \quad (4.13)$$

where

$$\lambda = \frac{3a}{\delta}, \quad r = \cos\theta. \quad (4.14)$$

Even though the collocation technique mentioned above can also be used to solve (4.13), in this case perhaps a more appropriate technique would be to use a weighted residual method and reduce (4.13) to an infinite algebraic system. Thus, if we select the weight functions  $U_{2n}(r) \sqrt{1-r^2}$  and use the orthogonality conditions

$$\frac{1}{\pi} \int_{-1}^1 U_i(r) U_j(r) \sqrt{1-r^2} dr = \begin{cases} 0, & i \neq j \\ \frac{1}{2}, & i = j \end{cases} \quad (4.15)$$

(4.13) may be reduced to

$$A_i = \sum_1^{\infty} c_{ij} A_j + d_{i-1}, \quad i = 1, 2, \dots, \quad (4.16)$$

where

$$d_i = -\frac{2}{\pi} \int_{-1}^1 \sigma_0(r) U_{2i}(r) \sqrt{1-r^2} dr, \quad i = 0, 1, 2, \dots, \quad (4.17)$$

$$c_{ij} = \frac{2\lambda}{\pi} \left[ \frac{1}{(2i-2)^2 - (2j-1)^2} - \frac{1}{(2i)^2 - (2j-1)^2} \right]. \quad (4.18)$$

The infinite system (4.16) can be solved by reduction and convergence is assured provided the system is regular [12]. The condition for regularity is

$$\sum_{j=1}^{\infty} |c_{ij}| < 1, \quad i = 1, 2, \dots \quad (4.19)$$

Performing the infinite sum, (4.19) may be expressed as

$$\frac{2\lambda}{\pi} \left[ \frac{8(2i-1)}{(4i-3)(4i-1)} + 2 \sum_{j=1}^{i-2} \left( \frac{1}{(2i-2j)^2 - (2j-1)^2} - \frac{1}{(2i)^2 - (2j-1)^2} \right) \right] < 1. \quad (4.20)$$

In (4.20) the bracketed quantity is greatest for  $i = 1$ . Hence the condition of regularity becomes

$$\lambda < \frac{3\pi}{16} \quad \text{or} \quad \frac{3a}{\delta} < \frac{3\pi}{16}. \quad (4.21)$$

For  $\lambda > 3\pi/16$  the system is quasi-regular in the sense that there exist an  $i$  for which the infinite system beginning with the  $(i+1)$  st equation is regular.<sup>1</sup>

In the problem under consideration the physically important quantities are the crack opening displacement  $w(x,0)$  and the shear stress  $\sigma_{yz}(x,0)$  along the interface, particularly the stress intensity factor. From (2.21), (4.6) and (4.7)  $w(x,0)$  may easily be obtained as follows:

$$w(x,0) = \int_{-a}^x g(t) dt = -\frac{1}{\mu(0)} \sum_0^{\infty} \frac{1}{n} A_n U_{2n-2} \left( \frac{x}{a} \right) \sqrt{a^2 - x^2}, \quad |x| < a. \quad (4.22)$$

Referring to (2.23) and (2.27) it may be observed that the left hand side of the integral equation represents  $\sigma_{yz}(x,0)$  for  $|x| > a$  as well as for  $|x| < a$ . Thus, by substituting from (4.6) - (4.8) into (2.27), for  $x = ar$  and  $|r| > 1$  we obtain

<sup>1</sup>There seems to be a curious analogy between the antiplane shear problem for a half plane with the shear modulus given by (4.2) and the cover plate problem described in [13]. In [13] the cover plate was approximated by a membrane of thickness  $h$  and elastic constants  $\mu_1$  and  $\kappa_1$ , and  $\lambda$  was the stiffness parameter defined by  $\lambda = \mu_2 (1 + \kappa_1) / [2\mu_1 h (1 + \kappa_2)]$  where  $\mu_2$  and  $\kappa_2$  are the elastic constants of the substrate. In the two problems the analogous physical quantities are the interface shear stress  $\sigma_{xy}$  (in [13]) and  $\mu(0) \psi(s)$  (see (2.21) and (4.6)).

$$\begin{aligned}
\sigma_{yz}(x,0) &= \sum_0^{\infty} A_n \frac{1}{\pi} \int_{-1}^1 \left[ \frac{1}{s-r} + k(ar, as) \right] \frac{T_{2n-1}(s)}{\sqrt{1-s^2}} ds \\
&= - \sum_0^{\infty} A_n \frac{\left[ \frac{r|/r}{\sqrt{r^2-1}} \left[ r - \frac{|r|}{r} \sqrt{r^2-1} \right] \right]^{2n-1}}{\sqrt{r^2-1}} \\
&\quad + \frac{1}{\pi} \sum_0^{\infty} A_n \int_{-1}^1 k(ar, as) \frac{T_{2n-1}(s)}{\sqrt{1-s^2}} ds .
\end{aligned} \tag{4.23}$$

If we now define the mode III stress intensity factor  $k_3$  at the crack tip  $x = a$  by

$$k_3 = \lim_{x \rightarrow a+0} \sqrt{2(x-a)} \sigma_{yz}(x,0) . \tag{4.24}$$

from (4.23) it may easily be shown that

$$k_3 = -\sqrt{a} \sum_0^{\infty} A_n . \tag{4.25}$$

As a third example we consider one of the expressions found for  $\mu(y)$  in Section 3, namely

$$\mu(y) = \mu_0 \frac{\coth^2(\beta y + \delta)}{\coth^2 \delta} , \quad \mu'(y) = \mu_0 \frac{\tanh^2(\beta y + \delta)}{\tanh^2 \delta} , \quad \delta > 0, \quad 0 < \beta < \infty . \tag{4.26}$$

The problem is solved by simply replacing the kernels  $k_a$  or  $k_b$  given (4.3) or (4.4) by  $k_c$  found in Section 3 and by following the procedure outlined in this section.

## 5. Results and Discussion

Based on simple physical considerations it may be observed that the solution given in this study for a nonhomogeneous half plane having a shear modulus  $\mu(y)$ ,  $y > 0$ , is valid also for the corresponding infinite medium in which  $y = 0$  is a plane of material symmetry, that is,  $\mu(-y) = \mu(y)$ ,  $-\infty < y < \infty$ . Thus, in the examples considered if we let the material nonhomogeneity parameter  $\beta$  be zero in (4.1), (4.2) and (4.26),  $\mu$  becomes a constant  $\mu(0)$  and the problem reduces to that of a homogeneous plane having a crack which is subjected to symmetric crack surface tractions. In fact from

(2.17), (2.27) and (2.28) it may be seen that for  $\beta = 0$  we have  $\lambda = |\alpha|$  and  $\mu'(0) = 0$  giving  $k(x,t) = 0$ . For example, if  $\sigma_0(x) = -p_0$ , from (4.6) - (4.11) and (4.23) it follows that,

$$M_{2n-1} = 0, A_1 = -p_0, A_n = 0, (n > 1), g(x) = -\frac{p_0}{\mu_0} \frac{x}{\sqrt{a^2 - x^2}}, |x| < a,$$

$$\sigma_{yz}(x,0) = p_0 \left( \frac{|x|}{\sqrt{x^2 - a^2}} - 1 \right), k_3 = p_0 \sqrt{a}. \quad (5.1)$$

Similarly, observing that  $v^2 = \{U_1(r) + U_0(r)\}/4$ , for a parabolic traction  $\sigma_0(x) = -p_2(x/a)^2$  it may easily be seen that  $A_1 = A_2 = p_2/4$  and

$$\sigma_{yz}(x,0) = \frac{p_2/4}{\sqrt{x^2 - a^2}} \left[ x - \sqrt{x^2 - a^2} + a \left( \frac{x}{a} - \sqrt{\left(\frac{x}{a}\right)^2 - 1} \right)^3 \right], x > a. \quad (5.2)$$

giving  $k_3 = p_2 \sqrt{a}/2$  (see Table 1). Also, in the third example considered in Section 3, from (3.23) it is seen that for  $\beta = 0$   $k_3(x,t) = 0$  and (3.13) reduces to an integral equation for a homogeneous material having the shear modulus  $\mu(0)$ .

For a plane with various forms of nonhomogeneities considered in Sections 2 and 3 the calculated stress intensity factors are given in Tables 2 and 3. In these results  $p_0$  and  $p_2$  again refer to the loading parameters defined in Table 1. In a limited way the results for uniform loading are also displayed in Figures 2-4. The materials considered in these three examples exhibit some distinct features. The hyperbolic functions used in Table 2 and Fig. 2 to represent the shear modulus have constant asymptotic values for  $y \rightarrow \infty$ , namely  $\mu_0 / \tanh^2 \delta$  and  $\mu_0 / \coth^2 \delta$ , where  $\mu_0 = \mu(0)$  (see the insert in Fig. 2). In the parabolic distribution for  $\mu(y)$  assumed in Fig. 3 and Table 3, for  $\beta < 0$   $\mu$  becomes zero at  $y = \delta/\beta$  and hence the results correspond to a nonhomogeneous layer of finite thickness with vanishingly decreasing shear modulus away from the interface. For this reason in this example the stress intensity factors corresponding to  $\beta < 0$  are considerably greater than that of the other examples shown in Figures 2 and 4 and Tables 2 and 3 in which  $\mu(y)$  is also a monotonically decreasing function.

Let us now examine the asymptotic behavior of the stress intensity factor  $k_3$  as  $\beta \rightarrow \pm \infty$ . First, from (4.6), (4.7) and (4.25) it can be seen that  $k_3(a)$  may also be expressed in the following alternate form:

$$k_3(a) = -\lim_{x \rightarrow a} \mu(0) \sqrt{2(a-x)} g(x). \quad (5.3)$$

In the examples given in Table 3 and Figures 3 and 4, it may now be seen that as  $\beta \rightarrow +\infty$  the stiffness of the medium would increase indefinitely and, under loadings of finite magnitude, the crack opening displacement or  $g(x)$ , and consequently,  $k_3(a)$  would tend to zero. These physically expected trends may be observed in Figures 3 and 4 and in Table 3. Similarly in the example given in Table 3 and Fig. 4 for  $\mu(y) = \mu_0 \exp(2\beta y)$ , the stiffness of the medium would decrease indefinitely as  $\beta \rightarrow -\infty$ , and consequently  $k_3(a)$  would tend to infinity. Also, for  $\beta < 0$  and  $\mu(y)/\mu_0 = (\beta y + \delta)^2/\delta^2$  the "thickness" of the medium  $y_0 = -\delta/\beta$  and as a result its stiffness would decrease indefinitely as  $\beta \rightarrow -\infty$ , again causing  $k_3(a)$  to approach infinity.

The examples considered in Table 2 and Fig. 2 are quite different and somewhat more practical than the examples shown in Table 3 in that for  $\beta \rightarrow \infty$  the medium becomes homogeneous with a shear modulus  $\mu(0)/\coth^2 \delta$  or  $\mu(0)/\tanh^2 \delta$ . Thus, in the limiting case of  $\beta = \infty$  the stress intensity factor ought to be independent of the shear modulus and should have the values given in Table 1. This trend, of course, is not observed in Table 2 and Fig. 2. The explanation of the discrepancy may be found in the fact that, because of the discontinuous change taking place in  $\mu(0)$  at  $\beta = \infty$ , the only physical quantity that should be expected to vary continuously as  $\beta \rightarrow \infty$  is the strain energy release rate which may be defined by and expressed as

$$\mathcal{G} = \frac{dE_0}{da}, \quad dE_0 = \frac{1}{2} \int_a^{a+da} \sigma_{yz}(x,0) w(x-a,0) dx, \quad \mathcal{G} = \frac{\pi k_3^2(a)}{4\mu(0)} \quad (5.4)$$

where  $E_0$  is the externally added or internally released energy that is available for fracture. Physically the problem may be visualized as a crack problem for a homogeneous half plane bounded to a rigid substrate through a thin nonhomogeneous layer. The objective is to determine the asymptotic behavior of the solution as the layer thickness approaches zero.

To gain a better insight to the problem we consider the simpler example of piecewise homogeneous medium shown in Fig. 5. The mode III crack problem described by Fig. 5 is that of two identical homogeneous half spaces having the shear modulus  $\mu_2$  which are bonded through a homogeneous layer of shear modulus  $\mu_1$  and thickness  $2h$ . The layer contains a crack of length  $2a$  in the plane of the symmetry. Following a

technique described in section 2, the mixed boundary value problem may easily be reduced to the following singular integral equation [14]:

$$\frac{1}{\pi} \int_{-a}^a \left\{ \frac{1}{t-x} - \mu^* k_1(x, t) \right\} g(t) dt = \frac{\sigma_0(x)}{\mu_1}, \quad -a < x < a,$$

$$\mu^* = \frac{\mu_1 - \mu_2}{\mu_1 + \mu_2}, \quad k_1(x, t) = 2 \int_0^\infty \frac{e^{-2\alpha h}}{\mu^* e^{-2\alpha h} + 1} \sin \alpha(t-x) d\alpha \quad (5.5a, b)$$

First, we simply note that for  $h = \infty$  the problem becomes one of a cracked homogeneous plane with shear modulus  $\mu_1$  for which the solution is given by (5.1) and (5.2) and Table 1, specifically

$$\sigma_0(x) = -p_0: \quad \frac{k_3(a)}{p_0 \sqrt{a}} = 1, \quad \frac{\mathcal{G}(a)}{\mathcal{G}_0} = 1, \quad \mathcal{G}_0 = \frac{\pi p_0^2 a}{4\mu_1},$$

$$\sigma_0(x) = -p_2 \left(\frac{x}{a}\right)^2: \quad \frac{k_3(a)}{p_2 \sqrt{a}} = \frac{1}{2}, \quad \frac{\mathcal{G}(a)}{\mathcal{G}_1} = 0.25, \quad \mathcal{G}_1 = \frac{\pi p_2^2 a}{4\mu_1}, \quad (5.6a, b)$$

Referring to (5.4) we note that the strain energy release rate  $\mathcal{G}$  calculated in this article and given in various figures and tables and in equations (5.4), (5.6) and elsewhere correspond to one quarter of the total enwrqy released in a cracked medium such as that shown in Fig.5. In the other limiting case of  $h \rightarrow 0$  it may easily be shown that

$$k_1(x, t) \rightarrow \frac{\mu_1 + \mu_2}{\mu_1} \left( \frac{1}{t-x} \right) \quad (5.7)$$

and (5.5a) becomes

$$\frac{1}{\pi} \int_{-a}^a \frac{g(t)}{t-x} dt = \frac{\sigma_0(x)}{\mu_2}, \quad -a < x < a, \quad (5.8)$$

which is the integral equation for a homogeneous medium having the shear modulus  $\mu_2$ . Thus, from (5.8) it follows that

$$\sigma_0(x) = -p_0: \quad \frac{\mathcal{G}(a)}{\mathcal{G}_2} = 1, \quad \mathcal{G}_2 = \frac{\pi p_0^2 a}{4\mu_2} = \frac{\mu_1}{\mu_2} \mathcal{G}_0,$$

$$\sigma_0(x) = -p_2 \left(\frac{x}{a}\right)^2: \quad \frac{\mathcal{G}(a)}{\mathcal{G}_3} = 0.25, \quad \mathcal{G}_3 = \frac{\pi p_2^2 a}{4\mu_2} = \frac{\mu_1}{\mu_2} \mathcal{G}_1. \quad (5.9a, b)$$

Referring now to Fig.5, we observe that as long as  $h > 0$ , the stress intensity factor and the strain energy release rate are defined by

$$k_3(a) = -\lim_{x \rightarrow a} \mu(0) \sqrt{2(a-x)} g(x), \quad \mathcal{G}(a) = \frac{\pi k_3^2(a)}{4\mu_1}, \quad (5.10)$$

where  $g(x)$  is obtained from (5.5a). For the loading conditions given in Table 1 and for  $\mu_1/\mu_2 = 2$  and  $\mu_1/\mu_2 = 0.5$  these calculated results are given in Table 4 and are also partially shown in Fig.6. The limiting values of  $\mathcal{G}(a)$  for  $h \rightarrow \infty$  and  $h \rightarrow 0$  and  $k_3(a)$  for  $h \rightarrow \infty$  are clear and unambiguous and are given by (5.6) and (5.9), respectively. From (5.10) (5.9) and (5.6) it is also seen that for  $h = +0$

$$\begin{aligned} \mathcal{G}(a) &= \frac{\pi k_3^2(a)}{4\mu_1} = \mathcal{G}_2 = \frac{\pi p_0^2 a}{4\mu_2}, \quad k_3(a) = \sqrt{\frac{\mu_1}{\mu_2}} p_0 \sqrt{a}, \\ \mathcal{G}(a) &= \frac{\pi k_3^2(a)}{4\mu_1} = 0.25 = \mathcal{G}_3 = 0.25 \frac{\pi p_0^2 a}{4\mu_2}, \quad k_3(a) = \frac{1}{2} \sqrt{\frac{\mu_1}{\mu_2}} p_0 \sqrt{a}. \end{aligned} \quad (5.11a,b)$$

Table 4 and Fig.6 show that these are indeed the limiting values of the results obtained from (5.5a) and (5.10).

Considering the fact that for  $h \rightarrow 0$  the problem reduces to that of a homogeneous plane, the limiting value of  $k_3$  still appears to be somewhat paradoxical. The explanation of the apparent discontinuity in  $k_3$  at  $h = +0$  lies in the fact that for very small  $h$ ,  $k_3$  obtained from the integral equation (5.5a) and shown in Table 4 is the measure of near field quantities. Far field quantities should, of course, be that of the homogeneous infinite medium. Without a lengthy singular perturbation analysis this can be shown by examining, for example, the crack opening displacement  $w(x,0)$  very near the crack tip as  $h$  approaches zero. The results calculated from (5.5a), (4.5) and (4.22) are shown in Figures 7 and 8. Figures 7a and 8a show  $w(x,0)$  and  $G(x)$  for various values of  $\mu_1/\mu_2$  and  $h/a$ . From Fig. 7a it is seen that away from the crack tip as  $h \rightarrow 0$   $w(x,0)$  converges to the corresponding homogeneous infinite plane values (indicated by  $h = 0$ ). Fig. 7b shows a magnified version of  $w(x,0)$  near the crack tip for  $\mu_2/\mu_1 = 2$ . Note that  $w \sim p_0/\mu$ . The curves marked by  $(h/a = 0, \mu_2/\mu_1 = 2)$  and by  $\mu_1 = \mu_2$  are simple ellipses. As expected, away from the crack tip the curves marked by small nonzero values of  $h/a$  are seen to converge to  $h/a = 0$  ellipse. However, near the crack tip the behavior of these curves is quite different and as  $h \rightarrow 0$  they seem to have a

different slope than that of the corresponding ellipse. These may be seen somewhat better in Fig. 8 showing  $G(x)$ ,  $G(a)$  being the measure of  $k_3(a)$  (see Eq. (4.5)). From (5.10a) note that for  $h = 0$ , that is, for the homogeneous plane  $\mu = \mu_2$ ,  $k_3 = -\mu_2 G(a)/\sqrt{a}$ , whereas for  $h > 0$   $k_3 = -\mu_1 G(a)/\sqrt{a}$ . Hence, the straight line corresponding to  $h = 0$  gives

$$G(x) = -\frac{1}{2} \frac{p_0 x}{\mu_1} = -\frac{p_0 x}{\mu_2}, \quad k_3(a) = p_0 \sqrt{a}. \quad (5.12)$$

The values of  $G(a)$  for nonzero values of  $h$  shown in the figure give the stress intensity factors listed in Table 4. The figure shows that at  $h = +0$   $G(x)$  would have a spike the value of which seems to approach the independently calculated value of  $\sqrt{\mu_1/\mu_2}$ . The distribution of  $G(x)$  also shows the expected "pinching" of the crack opening displacement very near the crack tip, as exhibited by two inflexion points.

Figures 9 and 10 give some sample results showing the influence of the material nonhomogeneity parameter  $\beta$  on the crack opening displacement  $w(x,0)$ ,  $-a < x < a$ . As  $\beta$  increases, in both examples the material stiffness also increases. Consequently, in both cases the crack opening displacement is seen to decrease for increasing values of  $\beta$ .

Based on the results given in Tables 2 and 3 one may conclude that in fracture mechanics analysis involving nonhomogeneous materials the "crack driving force" (as measured by the stress intensity factors or the strain energy release rate) may differ quite considerably from the values given by the corresponding homogeneous materials. One may also note that in diffusion problems the square-root nature of the flux singularity at the crack tip is not influenced by the material nonhomogeneity.

Table 1. Loading conditions used and the corresponding stress intensity factors for  $a\beta=0$ .

$\sigma_0(x)$	$-p_0$	$-p_2(x/a)^2$
$k_3(a)$	$p_0\sqrt{a}$	$\frac{1}{2}p_2\sqrt{a}$

Table 2. The variation of stress intensity factors for various loading conditions shown in Table 1.,  $\delta = 1$ .

$$\mu(y)/\mu_0 = \frac{\coth^2(\beta y + \delta)}{\coth^2(\delta)} \quad \mu(y)/\mu_0 = \frac{\tanh^2(\beta y + \delta)}{\tanh^2(\delta)}$$

$\beta a$	$\frac{k_3}{p_0\sqrt{a}}$	$\frac{k_3}{p_2\sqrt{a}}$	$\frac{k_3}{p_0\sqrt{a}}$	$\frac{k_3}{p_2\sqrt{a}}$
0.0	1.00	0.5	1.00	0.5
0.1	1.028	0.508	0.972	0.492
0.2	1.049	0.514	0.951	0.486
0.4	1.081	0.524	0.922	0.476
0.5	1.093	0.528	0.911	0.473
0.6	1.104	0.524	0.901	0.469
0.7	1.114	0.534	0.893	0.466
0.8	1.123	0.538	0.886	0.464
0.9	1.131	0.541	0.879	0.462
1.0	1.138	0.543	0.874	0.459
1.5	1.167	0.554	0.853	0.450
2.0	1.187	0.562	0.839	0.444
2.5	1.202	0.569	0.828	0.439
3.0	1.214	0.575	0.821	0.434
4.0	1.231	0.584	0.810	0.428
10.0	1.276	0.611	0.783	0.408
$\infty$	1.313	0.657	0.762	0.381

Table 3. The variation of stress intensity factors for various loading conditions shown in Table 1.,  $\delta = 1$ .

$3a$	$\mu(y)/\mu_0 = \delta^{-2} (3y + \delta)^2$		$\mu(y)/\mu_0 = e^{23y}$	
	$\frac{k_3}{p_0\sqrt{a}}$	$\frac{k_3}{p_2\sqrt{a}}$	$\frac{k_3}{p_0\sqrt{a}}$	$\frac{k_3}{p_2\sqrt{a}}$
-1.0	5.48	1.562	1.481	0.636
-0.8	2.597	0.894	1.397	0.612
-0.6	1.775	0.698	1.308	0.587
-0.4	1.384	0.601	1.214	0.560
-0.2	1.153	0.542	1.113	0.532
-0.1	1.069	0.519	1.059	0.516
0.0	1.00	0.5	1.00	0.5
0.1	0.941	0.483	0.933	0.482
0.2	0.890	0.469	0.869	0.463
0.3	0.846	0.456	0.810	0.447
0.4	0.807	0.444	0.758	0.431
0.5	0.773	0.434	0.712	0.418
0.6	0.742	0.424	0.671	0.405
0.8	0.691	0.407	0.604	0.384
1.0	0.647	0.392	0.550	0.366
1.5	0.565	0.362	0.457	0.331
2.0	0.507	0.340	0.397	0.305
2.5	0.463	0.322	0.356	0.285
3.0	0.429	0.306	0.324	0.268

Table 4. The stress intensity factors and the strain energy release rates in two homogeneous half planes bonded through a homogeneous layer containing a crack (Fig. 5).

$h/a$	$\mu_1/\mu_2 = 2$				$\mu_1/\mu_2 = 1/2$			
	$\frac{k_3}{p_0 \sqrt{a}}$	$\frac{k_3}{p_2 \sqrt{a}}$	$\mathcal{G}/\mathcal{G}_0$	$\mathcal{G}/\mathcal{G}_1$	$\frac{k_3}{p_0 \sqrt{a}}$	$\frac{k_3}{p_2 \sqrt{a}}$	$\mathcal{G}/\mathcal{G}_0$	$\mathcal{G}/\mathcal{G}_1$
0.0	1.4142	0.7071	2.0	0.5	0.7071	0.3536	0.5	0.125
0.005	1.386	0.681	1.920	0.464	0.716	0.364	0.513	0.133
0.01	1.385	0.674	1.918	0.454	0.719	0.369	0.517	0.137
0.02	1.378	0.661	1.904	0.437	0.725	0.378	0.526	0.143
0.04	1.354	0.636	1.833	0.405	0.737	0.392	0.544	0.154
0.05	1.313	0.606	1.723	0.367	0.758	0.412	0.575	0.169
0.1	1.295	0.596	1.677	0.355	0.767	0.419	0.589	0.175
0.2	1.228	0.564	1.507	0.318	0.805	0.442	0.648	0.196
0.4	1.146	0.537	1.317	0.288	0.859	0.464	0.739	0.215
0.6	1.099	0.524	1.210	0.275	0.897	0.475	0.805	0.225
0.8	1.071	0.517	1.148	0.268	0.923	0.481	0.852	0.232
1.0	1.053	0.513	1.108	0.263	0.942	0.486	0.887	0.236
$\infty$	1.0	0.5	1.0	0.25	1.0	0.5	1.0	0.25

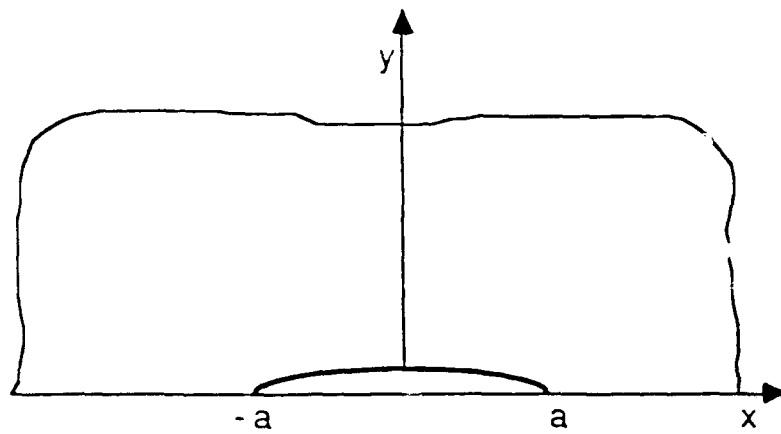


Fig.1. The geometry of the problem

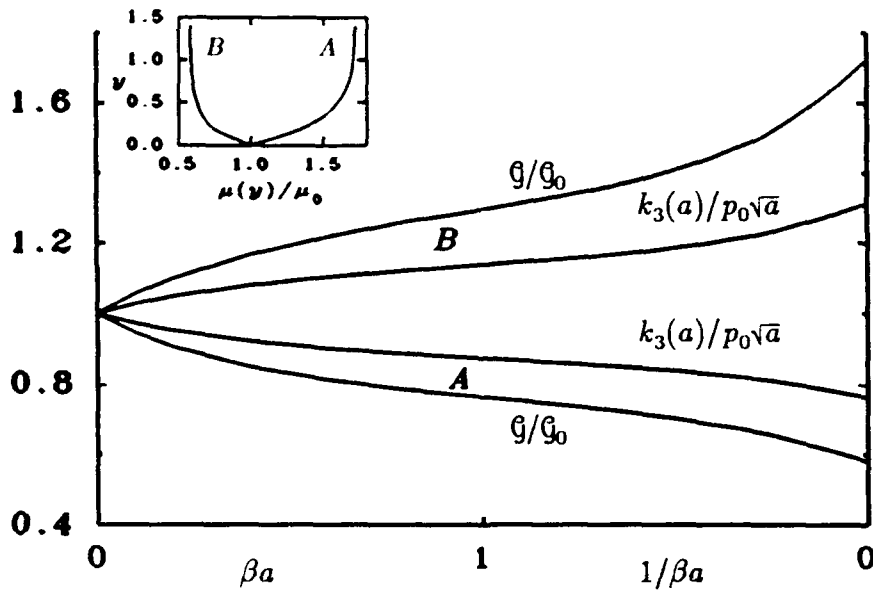


Fig.2. Stress intensity factor and Strain energy release rate for a nonhomogeneous half plane under uniform antiplane shear loading,  $\sigma_{yz}(x,0) = -p_0$ ,  $G_0 = \pi p_0^2 a / 4\mu_0$ ,

A:  $\mu(y) = \mu_0 \tanh^2(\beta y + \delta) / \tanh^2 \delta$ ,

B:  $\mu(y) = \mu_0 \coth^2(\beta y + \delta) / \coth^2 \delta$ ,  $\delta = 1$ .

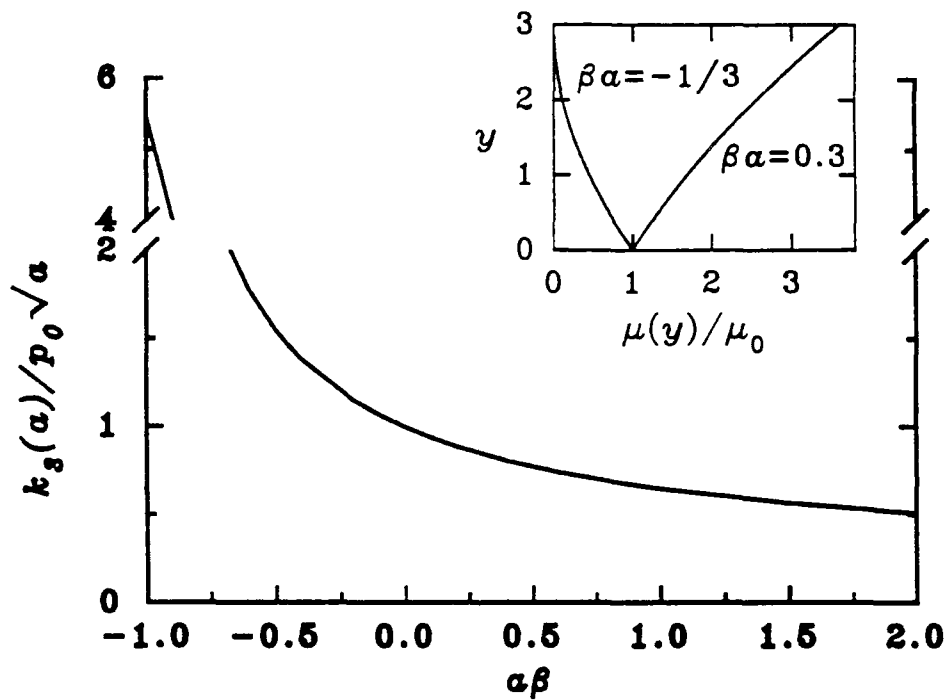


Fig.3 Stress intensity factor for a nonhomogeneous half plane subjected to uniform crack surface traction  $\sigma_{yz}(x,0) = -p_0$ , shear modulus  $\mu(y)/\mu_0 = (\beta y + \delta)^2/\delta^2$ ,  $\delta = 1$ .

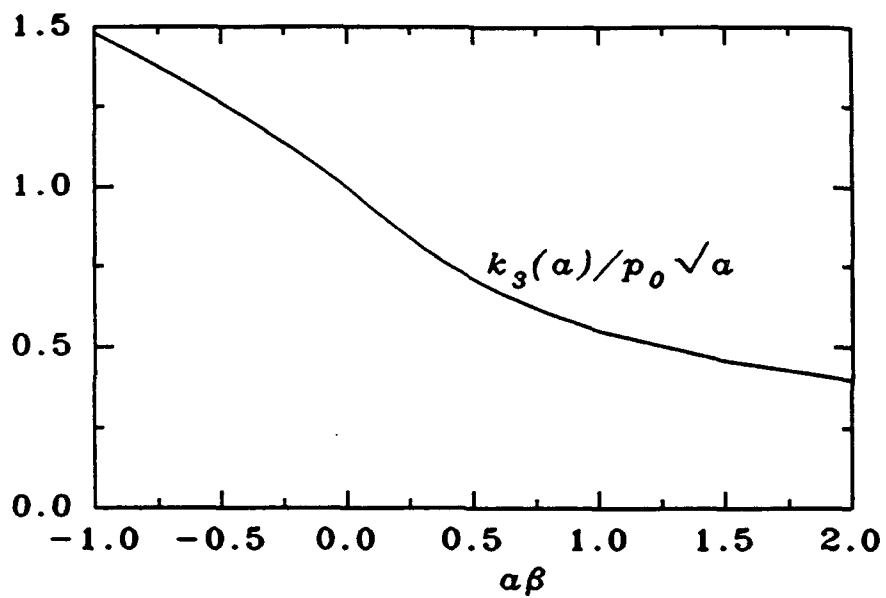


Fig.4 Stress intensity factor for a nonhomogeneous half plane subjected to uniform crack surface traction  $\sigma_{yz}(x,0) = -p_0$ ,  $\mu(y)/\mu_0 = e^{2\beta y}$ .

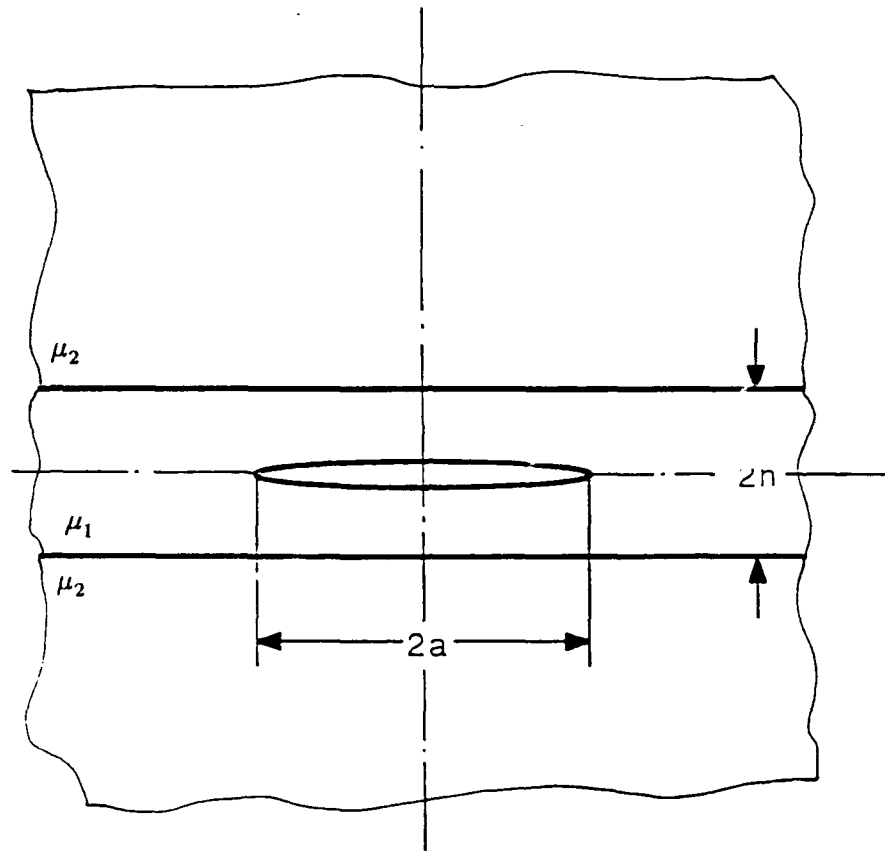


Fig.5 The symmetric mode III crack problem for two homogeneous half spaces bonded through a homogeneous elastic layer.

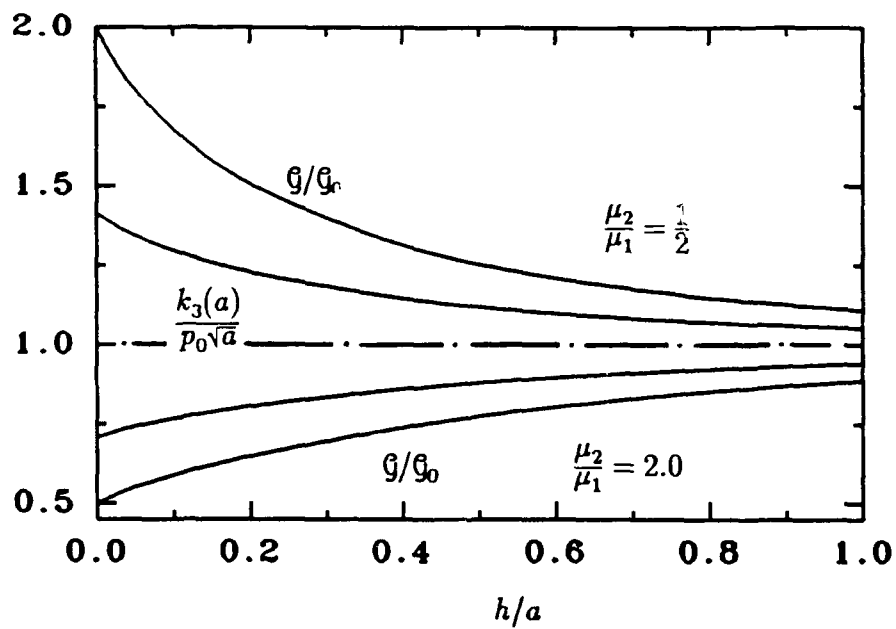


Fig. 6 Stress intensity factor and strain energy release rate as a function of layer thickness to crack length ratio ,  $G_0 = \pi p_0^2 a / 4\mu_1$ ,

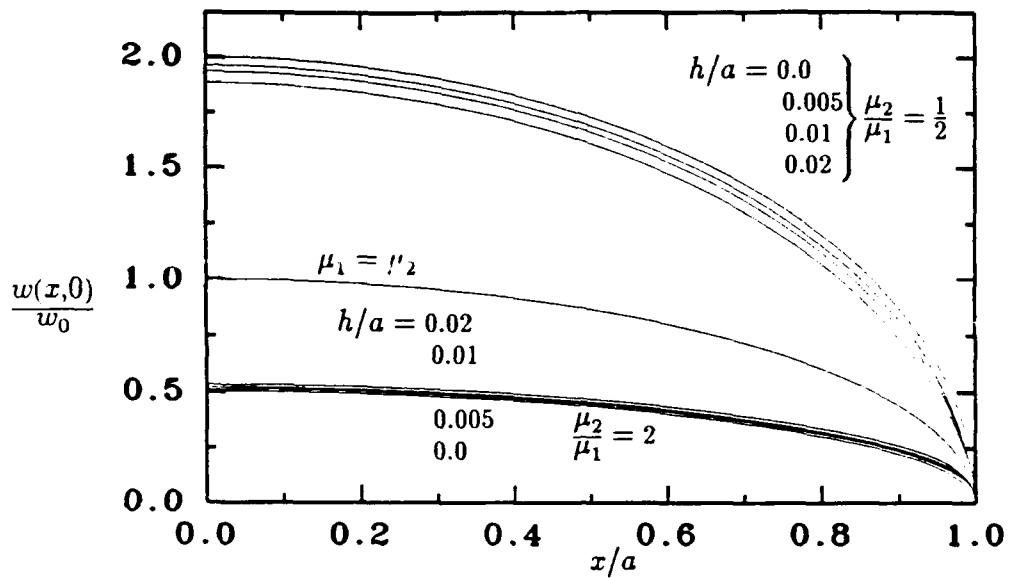


Fig.7a Crack surface displacement in a layer bonded to a semi-infinite homogeneous plane under uniform crack surface shear loading  $\sigma_{yz}(x,0) = -p_0$ ,  $w_0 = \frac{p_0 a}{\mu_1}$ .

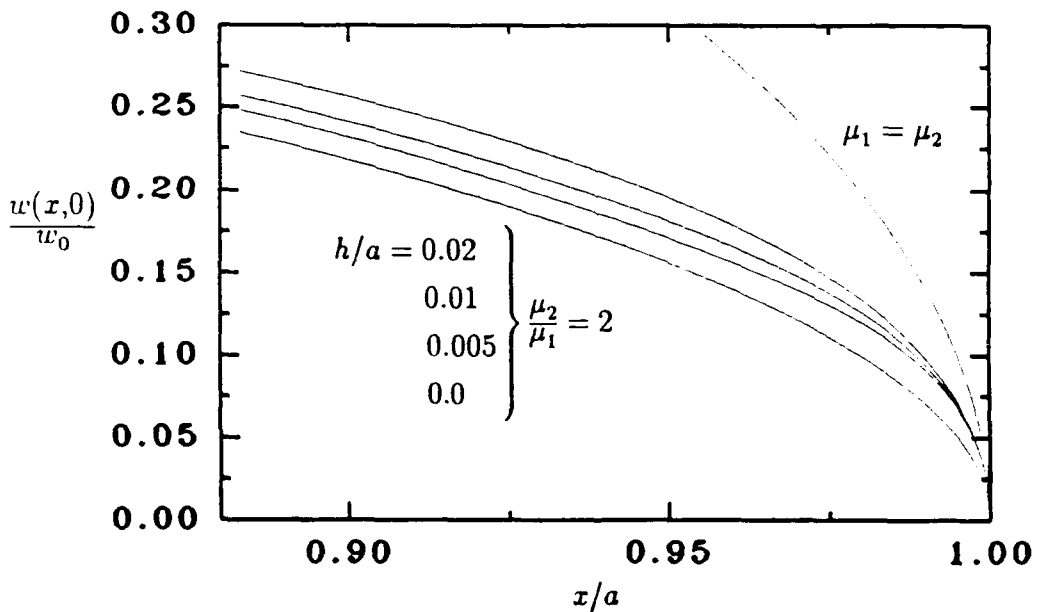


Fig.7b. Crack surface displacement in a layer bonded to a semi-infinite homogeneous plane under uniform crack surface shear loading  $\sigma_{yz}(x,0) = -p_0$ ,  $w_0 = \frac{p_0 a}{\mu_1}$ .

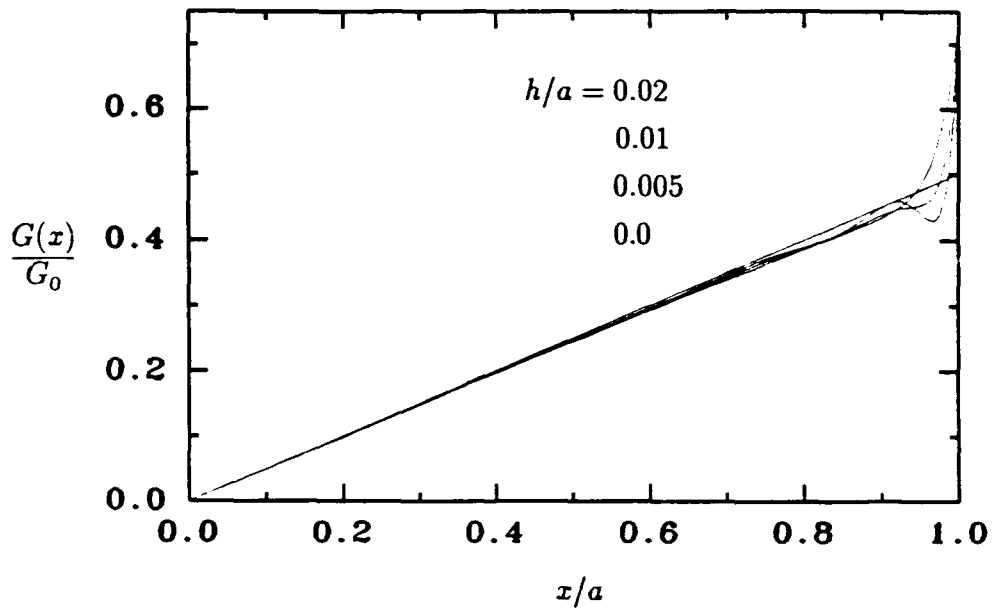


Fig.8a.  $G(x)$  vs  $x/a$ ,  $\mu_2/\mu_1 = 2.0$ ,  $G_0 = -p_0 a / \mu_1$ .

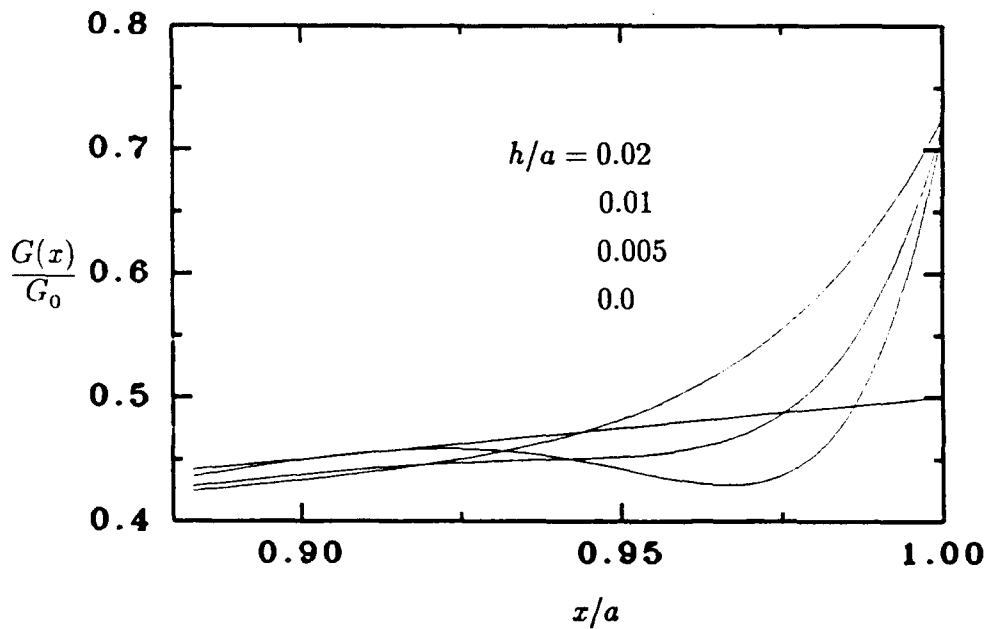


Fig.8b.  $G(x)$  vs  $x/a$ ,  $\mu_2/\mu_1 = 2.0$ ,  $G_0 = -p_0 a / \mu_1$ .

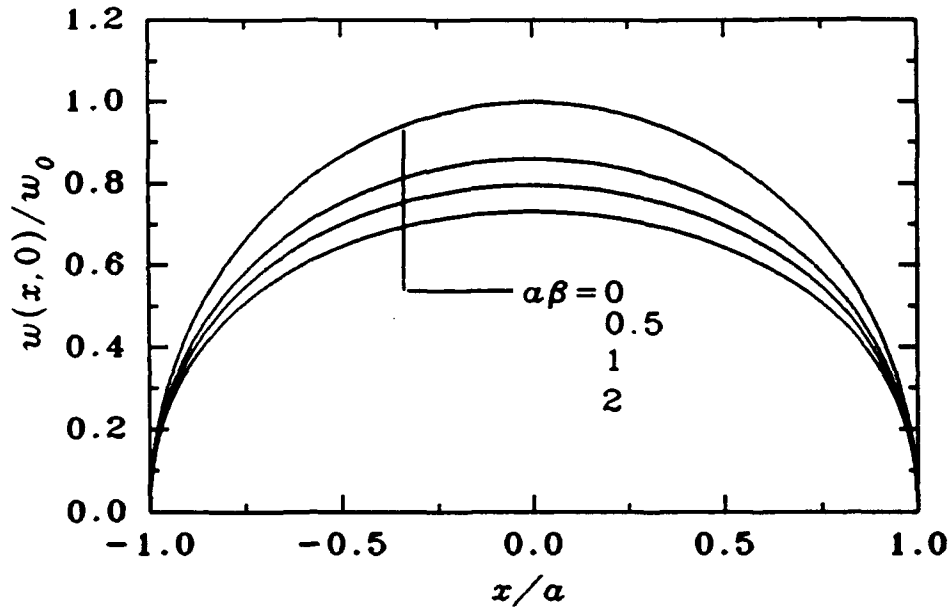


Fig. 1. Crack surface displacement in a semi-infinite nonhomogeneous plane under uniform crack surface shear loading  $\sigma_{yz}(x,0) = -p_0$ ;  $\mu(y)/\mu_0 = \tanh^2(\beta y + \delta)/\tanh^2(\delta)$ ,  $\delta = 1, w_0 = ap_0/\mu_0$ .

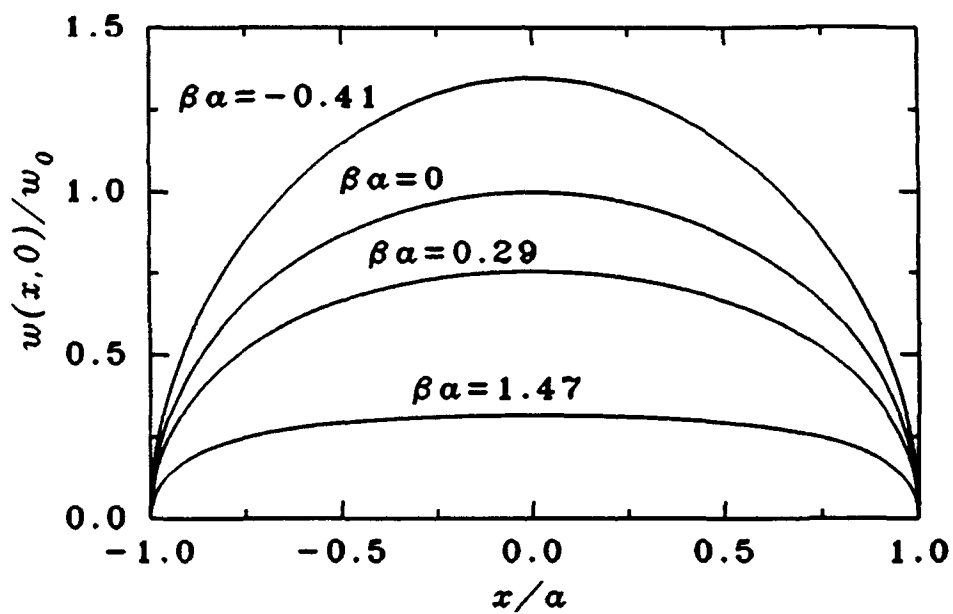


Fig.10 Crack surface displacement in a semi-infinite nonhomogeneous plane under uniform crack surface shear loading  $\sigma_{yz}(x,0) = -p_0$ ;  $\mu(y)/\mu_0 = e^{2\beta y}$ ,  $w_0 = ap_0/\mu_0$ .

Acknowledgements. This research was supported by ONR under the contract N00014-89-J-3188 and by NSF under the Grant MSS-8917867.

References

1. A.P. Batakis and J.W. Vogan, "Rocket Thrust Chamber Thermal Barrier Coatings." NASA CR-1750222, 1985.
2. D.L. Houck, ed. Thermal Spray: Advances in Coatings Technology, Proceedings of the Space National Thermal Spray Conference, Sept. 14-17, 1987, Orlando, FL. ASM International.
3. T. Hirano, T. Yamada, J. Teraki, M. Niino and A. Kumakawa, "A Study on a Functionally Gradient Material Design System for a Thrust Chamber." Proc. 16th Int. Symp. on Space Technology and Science, Sapporo, Japan, May 1988.
4. T. Hirano and T. Yamada, "Multi-Paradigm Expert System Architecture Based Upon the Inverse Design Concept," Int. Workshop on Artificial Intelligence for Industrial Applications, Hitachi, Japan, May 25-27, 1988.
5. M. Yamanouchi, M. Koizumi, T. Hirai and I. Shiota, ed. FGM '90, Proc. of 1st Int. Symp. on Functionally Gradient Materials, Functionally Gradient Materials Forum, Sendai, Japan, 1990.
6. K. Kerrihara, K. Sasaki and M. Kawarada, "Adhesion Improvement of Diamond Films." FGM '90, pp. 65-69, 1990.
7. A. Kawasaki and R. Watanabe, "Fabrication of Sintered Functionally Gradient Material by Powder Spray Forming Process," FGM '90, pp. 197-202, 1990.
8. M. Chigasaki, Y. Kojima, S. Nakashima and Y. Fukaya, "Partially Stabilized  $ZrO_2$  and Cu FGM Prepared by Dynamic Ion Mixing Process." FGM '90, pp. 269-272, 1990.
9. A. Kumakawa, M. Sasaki, M. Takahashi, M. Niino, N. Adachi and H. Arikawa, "Experimental Study on Thermomechanical Properties of FGMs at High Heat Fluxes," FGM '90, pp. 291-295, 1990.
10. E. Varley and B.A. Seymour, "A Method of Obtaining Exact Solutions to PDEs With Variable Coefficients," Studies in Appl. Math., Vol. 78, pp. 183-225, 1988.
11. N.I. Muskhelishvili, Singular Integral Equations, P. Noordhoff, Groningen, Holland, 1953.
12. L.V. Kantorovich and V.L. Krylov, Approximate Methods of Higher Analysis, Interscience, New York, 1958.
13. F. Erdogan and G.D. Gupta, "The Problem of an Elastic Stiffener Bonded to a Half Plane." J. Appl. Mech., Vol. 38, Trans. ASME, pp. 937-942, 1971.

14. F. Erdogan and G.D. Gupta, "The Stress Analysis of Multi-layered Composites with a Flaw", Int. J. Solids Structures, Vol.7, pp. 39-61,1971.